

1
2
3
4
5
6
7 Net Primary Production of
8
9
10 Terrestrial Ecosystems from 2000 to 2009
11
12
13

14
15 Christopher Potter ^{1*}
16

17 Steven Klooster ², Vanessa Genovese ²
18
19

20
21
22 ¹ NASA Ames Research Center, Moffett Field, CA
23

24 ² California State University Monterey Bay, Seaside, CA
25
26

27
28
29 Please return comments and other correspondence to:
30

31
32 * Corresponding author at
33

34 Email: chris.potter@nasa.gov
35

36
37 Tel. 650-604-6164; Fax. 650-604-4680
38
39
40
41
42
43
44
45
46
47
48
49
50
51
52
53
54
55
56
57
58
59
60
61
62
63
64
65

1
2
3
4 Abstract. The CASA (Carnegie-Ames-Stanford) ecosystem model has been used to
5
6 estimate monthly carbon fluxes in terrestrial ecosystems from 2000 to 2009, with global
7
8 data inputs from **NASA's Terra Moderate** Resolution Imaging Spectroradiometer
9
10 (MODIS) vegetation cover mapping. Net primary production (NPP) flux for atmospheric
11
12 carbon dioxide has varied slightly from year-to-year, but was predicted to have increased
13
14 over short multi-year periods in the regions of the high-latitude Northern Hemisphere,
15
16 South Asia, Central Africa, and the western Amazon since the year 2000. These CASA
17
18 results for global NPP were found to be in contrast to other recently published modeling
19
20 trends for terrestrial NPP with high sensitivity to regional drying patterns. Nonetheless,
21
22 periodic declines in regional NPP were predicted by CASA for the southern and western
23
24 United States, the southern Amazon, and southern and eastern Africa. NPP in tropical
25
26 forest zones was examined in greater detail to discover lower annual production values
27
28 than previously reported in many global models across the tropical rainforest zones, likely
29
30 due to the enhanced detection of lower production ecosystems replacing primary
31
32 rainforest.
33
34
35
36
37
38
39
40
41
42

43 Keywords: Terrestrial carbon, ecosystems, MODIS, NPP, drought
44
45
46
47
48
49
50
51
52
53
54
55
56
57
58
59
60
61
62
63
64
65

1. Introduction

Net photosynthetic accumulation of carbon by plants, also known as net primary production (NPP), provides the energy that drives most biotic processes on Earth. NPP represents much of the organic matter that is consumed by microbes and animals. Climate controls on NPP fluxes are an issue of central relevance to society, mainly because of concerns about the extent to which NPP in managed ecosystems can provide adequate food and fiber for a growing human population.

Previously published estimates of global NPP (Potter et al., 2003 and 2009; Nemani, 2003) imply that above-average global temperatures were commonly associated with an increasing trend in terrestrial ecosystem sinks for atmospheric CO₂ between the years 1982 and 1999. These predictions support the hypothesis that regional climate warming has had relatively small-scale positive impacts on atmospheric CO₂ sequestration rates, particularly in northern high latitude ecosystems (tundra and boreal forest). In the low latitude zones dominated by rainforests, the modeling results support the hypothesis that both sunlight and precipitation remain co-limitations to long-term NPP patterns. The trend in global terrestrial NPP since the year 1999 has become a subject of debate, with evidence to suggest a periodic downward trajectory linked to large-scale warming and drying in the Southern Hemisphere that counteracted increased NPP over the Northern Hemisphere (Zhao and Running, 2010).

Direct input of satellite vegetation index “greenness” data from the MODIS sensor into ecosystem simulation models can be used to estimate spatial variability in monthly NPP, plant biomass accumulation, and litter fall inputs to soil carbon pools (Potter et al., 1993 and 2009).

Global NPP of vegetation is predicted using the relationship between greenness reflectance properties and the fraction of absorption of photosynthetically active radiation (fPAR), assuming that net conversion efficiencies of PAR to plant carbon can be approximated for different ecosystems or are nearly constant across all ecosystems (Nemani and Running, 1989; Sellers et al., 1994; Goetz and Prince, 1998; Running and Nemani, 1998). For this study, we used MODIS collection 5 of the Enhanced Vegetation Index (EVI; Huete, et al., 2002 and 2006) as an improvement in the model inputs for PAR interception, aggregated to 0.5° (latitude/longitude) spatial resolution.

The CASA (Carnegie-Ames-Stanford) ecosystem model described in this study predicts NPP and terrestrial carbon balance on a global scale (Potter et al., 1993 and 2009). MODIS EVI data were direct input drivers for CASA. The purpose of this paper was to validate and report the patterns of regional variations in NPP in response to climate anomalies and extremes over the years 2000 to 2009.

2. Modeling Methods

Interannual NPP fluxes from the CASA model have been reported previously (Behrenfeld et al., 2001) and validated against multi-year estimates of NPP from field stations and tree rings (Malmström et al., 1997). Net ecosystem fluxes of carbon from CASA have been validated against atmospheric inverse model estimates over two decades (Potter et al., 2003).

As documented in Potter (1999), the monthly NPP flux, defined as net fixation of CO₂ by vegetation, is computed in CASA on the basis of light-use efficiency (Monteith, 1972). Monthly production of plant biomass is estimated as a product of time-varying surface solar irradiance, S_r , and EVI from the MODIS sensor, plus a constant light utilization efficiency term (e_{max}) that is modified by time-varying stress scalar terms for temperature (T) and moisture (W) effects (Equation 1).

$$NPP = S_r EVI e_{max} T W \quad (1)$$

The CASA e_{max} term was set uniformly at 0.55 g C MJ⁻¹ PAR, a value that derives from calibration of predicted annual NPP to previous field estimates (Potter et al., 2003). This model calibration has been calibrated globally by comparing predicted annual NPP to more than 1900 field measurements of NPP (Potter et al., 2003). Climate drivers for the CASA model were from the National Center for Environmental Prediction (NCEP) DOE-II reanalysis data set (Zhao and Running, 2010). NCEP land surface temperature, precipitation rates, and surface solar radiation data sets were averaged to monthly values at the 0.5° cell size. Land cover settings were aggregated from the MODIS global 1-km product (Zhao and Running, 2010).

The global 0.5° resolution MODIS vegetation index (VI) data sets used as inputs to Equation 1 were generated by aggregating monthly 0.05° (~6 km) data (MOD13C2 version 005) from the USGS Land Processes data center (LP DAAC). The VI layer was selected from each MOD13C2 spatial composite file and surface water values are converted to “NoData”. To aggregate from a 0.05° cell size to 0.5°, the VI values for each 10x10 pixel block were then

1
2
3
4 averaged to create a single 0.5° pixel greenness value. Each monthly layer was then multiplied
5
6 by 0.0001 to scale the data to the standard MODIS VI value range. This aggregation procedure
7
8 provided the greatest assurance of high-quality, cloud-free VI inputs to the carbon cycle model.
9
10 The MOD13C2 gap-filling and temporal smoothing procedures are commonly accepted methods
11
12 for unifying multi-year satellite VI data sets in cloudy regions (Jönsson and Eklundh, 2004). In
13
14 order to calculate annual CASA NPP, these procedures must be applied to fill cloud- (or aerosol-
15
16) contaminated observations, since plant photosynthesis continues during daylight hours
17
18 regardless of cloud cover (Zhao and Running, 2011).
19
20
21
22
23
24
25

26 The T stress scalar in Equation 1 was computed with reference to derivation of optimal
27
28 temperatures (T_{Opt}) for plant production. The T_{Opt} setting will vary by latitude and longitude,
29
30 ranging from just above 0° C in the Arctic to the middle thirties in low latitude deserts. The W
31
32 stress scalar was estimated from monthly water deficits, based on a comparison of moisture
33
34 supply (precipitation and stored soil water) to potential evapotranspiration (PET) demand using
35
36 the method of Priestly and Taylor (1972).
37
38
39
40
41
42
43

44 Evapotranspiration was connected to water content in the soil profile layers, according to
45
46 algorithms described by Potter (1999). The soil model design includes three-layer heat and
47
48 moisture content computations: surface organic matter, topsoil (0.3 m), and subsoil to rooting
49
50 depth (1 to 10 m). Maximum rooting depth for cropland and grassland cover types was set at 1
51
52 m, whereas non-tropical forest was set at 2 m and tropical forest was set at 10 m (Potter et al,
53
54 2003). These layers can differ in soil texture, moisture holding capacity, and carbon-nitrogen
55
56 dynamics. Water balance in the soil was modeled as the difference between precipitation or
57
58
59
60
61
62
63
64
65

1
2
3
4 volumetric percolation inputs, monthly estimates of PET, and the drainage output for each layer.
5
6 Inputs from rainfall can recharge the soil layers to field capacity. Excess water percolates
7
8 through to lower layers and may eventually leave the system as seepage and runoff.
9
10

11
12
13
14 The CASA model's seasonal NPP results were evaluated in this study using flux
15
16 estimates from eddy-correlation analysis, obtained from AmeriFlux tower flux sites that could
17
18 meet certain criteria for model comparisons. First, at least three complete years of site flux
19
20 measurements were required to evaluate model predictions of interannual variations in CASA
21
22 NPP fluxes. Second, winter (or dormant/dry) season NPP fluxes were required from a site to
23
24 evaluate model predictions on a year-round basis. Third, tower sites had to be representative of
25
26 the same (predominant) vegetation class setting in the global land cover data used as input to the
27
28 CASA model.
29
30
31
32
33
34
35

36 For sites meeting all of these criteria, AmeriFlux data sets were obtained from the central
37
38 data repository located at the Carbon Dioxide Information Analysis Center (CDIAC;
39
40 <http://public.ornl.gov/ameriflux/dataproducts.shtml>). Level 4 AmeriFlux records contained gap-
41
42 filled and ustar filtered records, complete with calculated gross productivity and total ecosystem
43
44 respiration terms on varying time intervals including hourly, daily, weekly, and monthly with
45
46 flags for the quality of the original and gap-filled data. NPP fluxes were computed from Level 4
47
48 estimates of gross primary production (GPP) by adjustment within an uncertainty range of 40-
49
50 50% of annual GPP carbon flux for temperate ecosystems (Waring et al., 1998; Zhang et al.,
51
52 2009) and 30% GPP in tropical forest ecosystems (Box et al., 2004). The uncertainties in the
53
54 ratio of tower-measured GPP to NPP may be even greater when monthly climate patterns are
55
56
57
58
59
60
61
62
63
64
65

considered, although there are no published studies available that address this seasonal variation factor for numerous tower sites.

3. Results

3.1. CASA Model Validation

For this latest CASA model application, a comparison of observed NPP ($n = 1927$) from field based measurements to predicted annual values from the CASA model was made to provide validation of terrestrial NPP predictions across all ecosystem types. Observed NPP values were compiled for the Ecosystem Model-Data Intercomparison (EMDI) activity by the Global Primary Productivity Data Initiative (GPPDI) working groups of the International Geosphere Biosphere Program Data and Information System (IGBP-DIS; Olson et al., 1997). Monthly MODIS EVI inputs resulted in a highly significant correlation ($R^2 = 0.90$) and a close 1:1 match of observed to CASA predicted NPP values, with the year 2001 selected as an example (Fig. 1.).

In this comparison to observed NPP, the CASA model was also tested for sensitivity to the vegetation index monthly time series as well by driving the NPP algorithm separately with either MODIS-EVI or MODIS-FPAR monthly inputs, holding climate inputs constant. A lower level of saturation in the low-to-medium range of plant production estimated from CASA modeling with EVI inputs compared to FPAR inputs was discovered by comparison of the two scatter plots over the range of annual NPP from 100-300 g C m⁻² yr⁻¹ (Fig. 1). Not only did EVI

1
2
3
4 result in less overall scatter in the predicted versus observed plot (i.e., $R^2 = 0.81$ using MODIS
5
6 FPAR inputs), the match to observed NPP in the high global range (of greater than 1000 g C m^{-2}
7
8 yr^{-1}) was markedly more consistent with EVI compared to MODIS FPAR inputs.
9
10

11
12
13
14 CASA NPP using EVI inputs was next compared across the tropical forest zones to a
15
16 literature review of NPP estimates by Clark et al. (2001) from old-growth tropical forest study
17
18 sites that attempted to create a consistent data set on NPP for these primary (undisturbed)
19
20 ecosystems. Because NPP is composed of both aboveground and belowground forest
21
22 production, upper and lower bounds around total NPP were reported by Clark et al. (2001)
23
24 expressly to serve as benchmarks for validating biogeochemical models for this biome. The
25
26 results of this compilation showed 58% (22 out of 38) of sites estimated with mean annual NPP
27
28 lower than $1000 \text{ g C m}^{-2} \text{ yr}^{-1}$, and another 26% (10 sites) were estimated with mean annual NPP
29
30 lower than $1200 \text{ g C m}^{-2} \text{ yr}^{-1}$ (Fig. 2). The comparison with the distribution of CASA NPP
31
32 across the tropical forest zones indicated that large tracts ($> 6 \text{ km}^2$) of undisturbed rainforest with
33
34 annual NPP higher than $1000 \text{ g C m}^{-2} \text{ yr}^{-1}$ (10 tons C ha^{-1}) were nearly undetectable at the global
35
36 scale. Despite the fact that hundreds of CASA annual NPP values of greater than 1000 g C m^{-2}
37
38 yr^{-1} were predicted at isolated locations across all tropical forest regions of the world (indicating
39
40 that the model has no built-in upper limit for NPP in its formulation), these high rainforest NPP
41
42 cases (as reported by Clark et al., 2001) were extreme outliers in the global model distribution
43
44 and hence do not appear as significant totals in Fig 2.
45
46
47
48
49
50
51
52
53
54

55 By way of additional model validation in the tropical zone, comparison of CASA
56
57 seasonal NPP against measured totals from the Large-scale Biosphere-Atmosphere Experiment
58
59
60
61
62
63
64
65

1
2
3
4 in Amazonia (LBA) showed close agreement at the Tapajos (Pará) forest experimental site
5
6 (Potter et al., 2009). At the ZF2 Manaus forest site, Chambers et al. (2004) directly measured
7
8 respiration rates from live leaf, live wood, and forest soil surfaces to derive an indirect NPP flux
9
10 estimate of $900 \text{ g C m}^{-2} \text{ yr}^{-1}$. Annual NPP from CASA for this general area (2.5° S lat , 60° W
11
12 lon) around Manaus in Brazil varied between $782 - 871 \text{ g C m}^{-2} \text{ yr}^{-1}$ between 2000 and 2004.
13
14
15
16
17
18

19 Seasonal validation of CASA monthly NPP predictions from the MOD13C2 EVI data
20
21 values closest to the AmeriFlux tower location was conducted by comparison to eddy-correlation
22
23 monthly estimates of the corresponding NPP fluxes. It should be noted that the monthly MODIS
24
25 EVI values in practically every grid cell of the global CASA model will be influenced by
26
27 periodic land cover disturbances and areas of sparse vegetation cover, including development,
28
29 roads, water bodies, and other natural features. It was expected, therefore, that CASA model
30
31 NPP flux predictions would be systematically lower than tower measurements of these carbon
32
33 fluxes, since tower footprints tend to be far less affected by wildfire and other disturbances,
34
35 compared for instance to the surrounding MODIS grid cell area in which they are located.
36
37
38
39
40
41
42

43 A total of eight Ameriflux tower sites were found to meet the criteria cited in the methods
44
45 section above for comparison to CASA model NPP predictions (Fig. 3). CASA model
46
47 predictions closely followed the seasonal timing of Ameriflux tower measurements at each site,
48
49 with a linear regression correlation coefficient of $R^2 = 0.77$ for all sites combined (Fig. 4). As
50
51 expected, CASA predicted NPP underestimated by a modest level of 7% compared to all the
52
53 monthly NPP measured from the Ameriflux towers (at the setting of 40% annual GPP carbon
54
55 flux).
56
57
58
59
60
61
62
63
64
65

3.2. Predicted Global NPP Patterns

Predicted terrestrial NPP for the globe in 2009 was 50.05 Pg C, a total carbon flux in the middle of the range of previous vegetation NPP predictions of between 44 to 66 Pg C per year for the period 1982-1998 (Cramer et al., 1999). We estimate that global terrestrial NPP increased by +0.14 Pg C over the time period of 2000 to 2009, due almost entirely to a strong upward trend in the Northern Hemisphere (Fig. 5). Annual NPP was predicted to have increased between the years 2000 and 2007 in the regions of high-latitude ($> 50^{\circ}$ N) North America and Eurasia, and also in South Asia, West and Central Africa, and the western Amazon (Figs. 5 and 6).

This upward trend in high-latitude NPP was controlled by a combination of rapidly warming temperatures from 2004 to 2005 (Zhao and Running, 2010), and by elevated MODIS EVI patterns over the same period. Periodic declines in regional NPP were predicted for the southern United States, the southern Amazon, western Europe, southern and eastern Africa, and Australia (Fig. 7); the timing of negative NPP anomalies in each of these regions was associated with severe droughts and, in some cases, extreme heat waves (World Meteorological Organization, 2001-2009).

When global NPP predictions were broken down into 30° latitude zones, monthly air temperature was found to be highly correlated ($R^2 > 0.9$) with seasonal increases and decreases in

1
2
3
4 NPP at latitudes between 30° N and 90° N (Table 1). Monthly precipitation was found to be
5
6 more closely correlated ($R^2 > 0.8$) with seasonal increases and decreases in NPP than was air
7
8 temperature at latitudes between 30° N and 30° S, whereas EVI was closely correlated ($R^2 > 0.7$)
9
10 with monthly NPP in all latitude zones. Correlations between monthly EVI anomalies (2000-
11
12 2009) and predicted monthly NPP anomalies were significant in all latitude zones as well, which
13
14 implies that, across latitude zones, interannual NPP variations were most strongly controlled by
15
16 EVI inputs, compared to short-term variations in air temperature or precipitation.
17
18
19
20
21
22

23
24 Nonetheless, there were many instances of severe drought affecting terrestrial NPP on
25
26 local-to-regional scales across the globe during the period of 2000 to 2008, mainly in areas of the
27
28 central North America, Africa, Brazil, and China (Fig. 7). Beginning with major droughts in
29
30 Brazil, the Horn of Africa, the Middle East, Central and South Asia, and China in 2000 and
31
32 2001, these events were followed by most of North America, southern Africa, and Australia
33
34 experiencing record low precipitation amounts in 2002, 2003, and 2004. Large areas of Europe,
35
36 southern Africa, Brazil, and Paraguay were affected by severe droughts in 2005. From 2006
37
38 through 2008, much of the United States, eastern and southern Africa, China, and Australia
39
40 experienced continued deficits of precipitation.
41
42
43
44
45
46
47

48 Drought in the Amazon basin approached unprecedented levels in 2009 (and into 2010;
49
50 Lewis et al., 2011), and the impact on NPP was evident in the CASA model prediction of 2009
51
52 anomalies in excess of $-100 \text{ g C m}^{-2} \text{ yr}^{-1}$ in the central and western portions of the basin (Fig. 7).
53
54 This was seen in contrast to the impacts of the severe drought of 2005, which was predicted to
55
56
57
58
59
60
61
62
63
64
65

1
2
3
4 have impacted tropical forest NPP (with anomalies on the order of $-20 \text{ g C m}^{-2} \text{ yr}^{-1}$) mainly in the
5
6 eastern and in more isolated southwestern portions of the Brazilian Amazon.
7
8
9

10
11 A notable global difference of our CASA model estimates of NPP from those of previous
12
13 terrestrial carbon studies (Cramer et al., 1999) was the magnitude of tropical forest NPP.
14

15
16 Whereas these previously cited estimates of annual NPP across rainforest study sites that were
17
18 largely protected from human disturbance have commonly exceeded $900 \text{ g C m}^{-2} \text{ yr}^{-1}$ (Clark et
19
20 al., 2001), our CASA model for 2009 estimated an average NPP of $840 \text{ g C m}^{-2} \text{ yr}^{-1}$ in the South
21
22 American tropical region, an average of $805 \text{ g C m}^{-2} \text{ yr}^{-1}$ in the African tropical region, and an
23
24 average of $847 \text{ g C m}^{-2} \text{ yr}^{-1}$ in the South East Asian tropical region. Although hundreds of
25
26 annual NPP values of greater than $1000 \text{ g C m}^{-2} \text{ yr}^{-1}$ were estimated as well at isolated locations
27
28 across all three tropical forest regions of the world, the impact of deforestation and replacement
29
30 of forests by lower production tropical agricultural systems has been widely captured by the
31
32 MODIS EVI inputs to CASA since the year 2000.
33
34
35
36
37
38
39
40

41 Across the tropical rainforest zones, CASA NPP in 2009 totaled to $13.7 \text{ Pg C yr}^{-1}$,
42
43 accounting for nearly one-third (27%) of global terrestrial NPP. Of the three major tropical
44
45 rainforest regions, South America (80°W - 43°W) accounted for 47% of the zonal NPP total,
46
47 whereas Africa (13.5°W - 40°E) and Asia (73.5°E - 162.5°E) regions together accounted for
48
49 45% of the zonal NPP total (Table 2).
50
51
52
53
54
55
56
57

58 4. Discussion 59 60 61 62 63 64 65

1
2
3
4
5
6
7 The comparative sensitivity of MODIS EVI and FPAR results to the range of global
8
9 measured NPP values (Fig. 1) confirms previous reports (Huete et al., 2002; Xiao et al., 2006;
10
11 Colditz et al., 2007) that the global EVI time series has a higher dynamic response across the full
12
13 range of vegetated cover, does not saturate in medium-to-high biomass areas, and is less
14
15 susceptible to atmospheric interference, all in contrast to other vegetation indices used previously
16
17 in the CASA model. The lower level of saturation of low-to-medium range plant production
18
19 estimated from CASA modeling with MODIS EVI inputs (compared to MODIS FPAR inputs)
20
21 resulted in lower annual NPP in any tropical zones where primary forest has become increasing
22
23 mixed with degraded forest and converted agricultural land uses. This global trend of rainforest
24
25 destruction has been reported at rates exceeding 2.3% of remaining humid forest cover between
26
27 the years 2000 and 2005 (Hansen et al., 2008).
28
29
30
31
32
33
34
35

36 We note that the patterns in terrestrial NPP from CASA between the years 2000 and 2007
37
38 differed from the decreasing trend of -0.51 Pg C reported from the global MODIS NPP
39
40 algorithm (hereafter abbreviated MNA; Zhao and Running, 2010; Running et al., 2004), which
41
42 used satellite FPAR inputs and the same NCEP reanalysis data set as in the CASA model for
43
44 climate inputs. On a regional basis, our model results also differed from the MNA for 2000-
45
46 2009 (Zhao and Running, 2010), which reported that NPP in the tropical zones (23.5° S to 23.5°
47
48 N) explained 93% of variations in the global NPP. In contrast, with CASA we found that NPP in
49
50 the tropical zones explained only 50-60% of variations in the global NPP, whereas NPP in the
51
52 latitude zone between 30°N and 60°N could explain between 40% and 50% of variations in the
53
54 global NPP.
55
56
57
58
59
60
61
62
63
64
65

1
2
3
4
5
6
7 Notwithstanding the difference in the global trend of NPP between CASA and the
8
9 predictions from the MNA, the overall patterns of interannual variations in Northern and
10
11 Southern Hemisphere NPP anomalies were similar between the two model results. NPP
12
13 anomalies in the Northern Hemisphere were negative from 2000-2003 and then became strongly
14
15 positive from 2004-2008, closely following the $0.1^{\circ} \text{ yr}^{-1}$ surface-warming trend in the model
16
17 input data. NPP anomalies in the Southern Hemisphere were positive from 2000-2003 and then
18
19 turned negative between 2004-2008, with 2005 being the most strongly negative anomaly year.
20
21
22
23
24
25

26 The main difference between the two model predictions was the magnitude of NPP
27
28 interannual anomalies in the Southern Hemisphere, with those from the MNA estimated to
29
30 exceed those from the CASA model by a factor of more than ten in the years 2000, 2001, and
31
32 2005. We note that the MNA-estimated cumulative loss of 4 Pg C NPP in the Southern
33
34 Hemisphere annual NPP between the years 2000 and 2005 is roughly equivalent to total yearly
35
36 NPP over all the tropical forests of Asia (Table 2), and exceeds by a factor of two the estimated
37
38 global emission of carbon to the atmosphere from tropical forest fires during the strong El Nino
39
40 droughts of 1997-1998 (van der Werf et al., 2004). Criticism of Zhao and Running's (2010)
41
42 results by Medlyn, (2011) and Samanta et al. (2011) include remarks that sensitivity analysis,
43
44 evaluation of bias introduced by gap filling of satellite data, and generally weak correlations with
45
46 field observations would result in the reported negative global trend in NPP being insignificant.
47
48
49
50
51
52
53

54 The differences in these recent model results underscore the problem of how remotely
55
56 sensed models for terrestrial NPP should account for environment stresses, especially those that
57
58 affect plant autotrophic respiration. For instance, previous studies (Nepstad et al., 1994; Saleska
59
60
61
62
63
64
65

1
2
3
4 et al., 2003; Xiao et al., 2003; Ichii et al., 2007) have concluded that the setting of proper rooting
5
6 depths is important to simulating primary production seasonality in tropical forests. The CASA
7
8 model specifies deep-rooting for prolonged tropical forest access to stored soil water and relies
9
10 on observed changes in MODIS EVI to track moisture stress effects globally. CASA does not
11
12 account for the additional costs of autotrophic respiration in the manner of the MNA. NPP
13
14 models such as the MNA do not consider rooting depth, but rely on nonlinear functions of
15
16 increasing temperature to estimate production responses to water scarcity. Such functions can
17
18 amplify heat stress effects greatly in the low-latitude zones, since the same increase in air
19
20 temperature at higher temperature bases in the tropics will increase autotrophic respiration costs
21
22 for NPP to greater degree than in the high latitude zones (Zhao and Running, 2010).
23
24
25
26
27
28
29
30

31 The different approaches to modeling environment controls on NPP cited in this paper
32
33 call attention to the need for additional measurements of terrestrial production in forested
34
35 landscapes of the world that have been impacted by deforestation and conversion to lower
36
37 production ecosystems. Terrestrial biosphere representations at coarse (1-km or greater)
38
39 geographic resolution cannot readily capture the vast areas of mixed non-forest uses within the
40
41 predominant land cover setting, and instead tend to treat tropical forest cover as if there were
42
43 continuous stands of intact trees with high potential respiration costs to primary production.
44
45
46
47
48
49

50 The reality is that forests are comprised of diverse mosaics of vegetation types with
51
52 widely varying photosynthetic and respiratory physiologies. Although the impacts of warming-
53
54 associated drought must not be overlooked as a periodic driver of carbon losses from ecosystems
55
56 to the atmosphere, forests of the world that have already been widely converted and degraded by
57
58
59
60
61
62
63
64
65

human use require far more field research to understand how to best represent these regions in global NPP models.

Acknowledgments. This work was supported by the Planetary Skin Institute and grants from NASA programs in Carbon Cycle Science and the Large-scale Biosphere-Atmosphere Experiment in Amazonia (LBA),

References

- Behrenfeld, M. J., J. T. Randerson, C. R. McClain, G. C. Feldman, S. Q. Los, C. I. Tucker, P. G. Falkowski, C. B. Field, R. Frouin, W. E. Esaias, D. D. Kolber, and N. H. Pollack, 2001. Biospheric primary production during an ENSO transition. *Science* 291, 2594-2597.
- Box, E. O., 2004 Gross production, respiration and biosphere CO₂ fluxes under global warming, *Tropical Ecology* 45(1): 13-29.
- Chambers, J. Q., E. S. Tribuzy, L. C. Toledo, B. F. Crispim, N. Higuchi, J. dos Santos, A. C. Araujo, B. Kruijt, A. D. Nobre, and S. E. Trumbore. 2004. Respiration from a tropical forest ecosystem: Partitioning of sources and low carbon use efficiency. *Ecological Applications* 14: S72-S88.
- Clark D A, Brown S, Kicklighter D W, Chambers J Q, Thomlinson J R, Ni J, Holland E A, 2001, Net primary production in tropical forests: an evaluation and synthesis of existing field data. *Ecological Applications*, 11, 371–384.
- Colditz, R.R., Conrad, C., Wehrmann, T., Schmidt, M. and Dech, S.W., 2007. Analysis of the quality of collection 4 and 5 vegetation index time series from MODIS. ISPRS Spatial Data Quality Symposium, Enschede, The Netherlands, CRC press.
- Cramer, W., Kicklighter, D. W., Bondeau, A.; Iii, B. Moore, Churkina, G.; Nemry, B.; Ruimy, A., Schloss, A. L., 1999, Comparing global models of terrestrial net primary productivity (NPP): overview and key results. *Global Change Biology*, 5, 1-15.
- Goetz, S. J, and S. D. Prince, 1998, Variability in light utilization and net primary production in boreal forest stands. *Canadian Journal of Forest Research*. 28: 375-389.
- Hansen, M.C., Roy, D., Lindquist, E., Justice, C.O., and Altstaad, A., 2008, A method for integrating MODIS and Landsat data for systematic monitoring of forest cover and

- change in the Congo Basin. *Remote Sens. Environ* 112:2495–2513.
- Huete, A., Didan, K., Miura, T., & Rodriguez, E., 2002. Overview of the radiometric and biophysical performance of the MODIS vegetation indices. *Remote Sens. Environ.*, 83, 195 – 213.
- Huete, A. R., K. Didan, Y. E. Shimabukuro, P. Ratana, S.R. Saleska, L.R. Hutya, D. Fitzjarald, W. Yang, R.R. Nemani, and R. Myneni, 2006, Amazon rainforests green- up with sunlight in dry season, *Geophys. Res. Lett.*, 33, L 06405, doi:10.1029/2005GL025583.
- Ichii, K., H. Hashimoto, M.A. White, C. Potter, L.R. Hutya, A.R. Huete, R.B. Myneni, R.R. Nemani, 2007, Constraining rooting depths in tropical rainforests using satellite data and ecosystem modeling for accurate simulation of GPP seasonality, *Global Change Biology*, 13, 67-77.
- Jönsson, P. and L. Eklundh, 2004, TIMESAT: A program for analysing time-series of satellite sensor data. *Comput. Geosci.* 30, 833.
- Lewis, S. L., P. M. Brando, O. L. Phillips, G. M. F. van der Heijden, and D. Nepstad, 2011, The 2010, Amazon drought, *Science*, 331(6017), 554, doi:10.1126/science.1200807.
- Malmström, C. M., M. V. Thompson. G. P. Juday, S. O. Los, J. T. Randerson, and C. B. Field, 1997. Interannual variation in global scale net primary production: Testing model estimates. *Global Biogeochem. Cycles.* 11, 367-392.
- Medlyn, B. E., 2011, Comment on “Drought-Induced reduction in Global Terrestrial Net Primary Production from 2000 Through 2009”. *Science*, 333, 1093.

- 1
2
3
4 Monteith, J. L., 1972, Solar radiation and productivity in tropical ecosystems. *Journal of Applied*
5
6 *Ecology*, 9, 747-766.
7
8
- 9 Nemani, R. R. and S.W. Running, 1989, Testing a theoretical climate-soil-leaf area
10
11 hydrologic equilibrium of forests using satellite data and ecosystem simulation, *Agric.*
12
13 *For. Met.*, 44, 245-260.
14
15
- 16 Nemani, R. R., C. D. Keeling, H. Hashimoto, W. M. Jolly, S. C. Piper, C. J. Tucker, R. B.
17
18 Myneni, and S. W. Running, 2003, Climate driven increases in global terrestrial net
19
20 primary production from 1982 to 1999. *Science*. 300, 1560-1563.
21
22
23
- 24 Nepstad, D. C., et al., 1994, The role of deep roots in the hydrological and carbon cycles of
25
26 Amazonian forests and pastures, *Nature*, 372, 666 – 669.
27
28
29
- 30 Olson, R. J., J. M. O. Scurlock, W. Cramer, W. J. Parton, and S. D. Prince, 1997, *From Sparse*
31
32 *Field Observations to a Consistent Global Dataset on Net Primary Production*. IGBP-
33
34 DIS Working Paper No. 16, IGBP-DIS, Toulouse, France, 1997.
35
36
37
38
- 39 Potter, C., S. Klooster, A. Huete, V. Genovese, M. Bustamante, L. Guimaraes Ferreira, R. Cosme
40
41 de Oliveira Junior, and R. Zepp, 2009, Terrestrial carbon sinks in the Brazilian Amazon
42
43 and Cerrado region predicted from MODIS satellite data and ecosystem modeling,
44
45 *Biogeosciences*, 6, 1–23.
46
47
- 48 Potter, C. S., 1999, Terrestrial biomass and the effects of deforestation on the global carbon
49
50 cycle. *BioScience*. 49, 769-778.
51
52
53
- 54 Potter, C., S. Klooster, R. Myneni, V. Genovese, P. Tan, V. Kumar, 2003 Continental scale
55
56 comparisons of terrestrial carbon sinks estimated from satellite data and ecosystem
57
58 modeling 1982-98. *Global and Planetary Change*, 39, 201-213.
59
60
61
62
63
64
65

- Potter, C. S., S. A. Klooster, and V. Brooks, 1999, Interannual variability in terrestrial net primary production: Exploration of trends and controls on regional to global scales, *Ecosystems*, 2, 36-48.
- Potter, C. S., J. T. Randerson, C. B. Field, P. A. Matson, P. M. Vitousek, H. A. Mooney, and S. A. Klooster, 1993, Terrestrial ecosystem production: A process model based on global satellite and surface data, *Global Biogeochem. Cycles*, 7, 811-841.
- Running, S. W., R. R. Nemani, F. A. Heinsch, M. Zhao, M. Reeves and H. Hashimoto. 2004. A continuous satellite-derived measure of global terrestrial primary production. *BioScience*, 54: 547-560.
- Running, S. W, and R. R. Nemani, 1998, Relating seasonal patterns of the AVHRR vegetation index to simulated photosynthesis and transpiration of forests in different climates. *Remote Sensing of Environment*. 24, 347-367.
- Saleska, S.R., S.D. Miller, D.M. Matross, M.L. Goulden, S.C. Wofsy, H. da Rocha, P.B. de Camargo, P.M. Crill, B.C. Daube, C. Freitas, L. Hutya, M. Keller, V. Kirchhoff, M. Menton, J.W. Munger, E.H. Pyle, A.H. Rice, H. Silva, 2003. Carbon in Amazon forests: unexpected seasonal fluxes and disturbance-induced losses. *Science*. 302: 1554-1557.
- Samanta, A., M. H. Costa, E.L. Nunes, S. A. Vieira, L. Xu, R. B. Myneni, 2011, Comment on “Drought-Induced reduction in Global Terrestrial Net Primary Production from 2000 Through 2009”. *Science*, 333, 1093.
- Sellers, P. J., C. J. Tucker, G. J. Collatz, S. O. Los, C. O. Justice, D. A. Dazlich, and D. A. Randall, 1994, A global 1x1 NDVI data set for climate studies. Part 2: the generation of global fields of terrestrial biophysical parameters from the NDVI. *International Journal of Remote Sensing*. 15, 3519-3545.

- van der Werf, G.R., J.T. Randerson, G.J. Collatz, L. Giglio, P.S. Kasibhatla, A. Arellano, S.C. Olsen, and E.S. Kasischke, 2004, Continental-scale partitioning of fire emissions during the 97/98 El Nino, *Science*, 303, 73-76.
- Waring, R. H., J. J. Landsberg and M. Williams, 1998, Net primary production of forests: a constant fraction of gross primary production? *Tree Physiol.* 18 (2): 129-134.
- World Meteorological Organization, WMO Statement on the Status of the Global Climate in 2001, WMO#670, December 18, 2001.
- Xiao, X.; Hagen, S.; Zhang, Q.; Keller, M.; Moore III, B., 2006. Detecting leaf phenology of seasonally moist tropical forests in South America with multi-temporal MODIS images.. *Remote Sens. Environ.*, 103 :465– 473.
- Xiao, X., Q. Zhang, S.R. Saleska, L. Huttyra, P. Camargo, S. Wofsy, S. Froking, S. Boles, M. Keller and B. Moore III. 2003, Satellite-based modeling of gross primary production in a seasonally moist tropical evergreen forest. 2005. *Remote Sens. Environ.*, 94: 105–122.
- Zhang, Y., M. Xu, H Chen, and J. Adams, 2009, Global pattern of NPP to GPP ratio derived from MODIS data: effects of ecosystem type, geographical location and climate, *Global Ecol. Biogeogr.*, 18, 280–290.
- Zhao, M. and S. W. Running, 2010, Drought-induced reduction in global terrestrial net primary production from 2000 through 2009, *Science*, 329, 940-943. Supporting Online Material at <http://www.sciencemag.org/content/329/5994/940/suppl/DC1>
- Zhao, M., and S. W. Running, 2011, Response to Comments on "Drought-Induced Reduction in Global Terrestrial Net Primary Production from 2000 Through 2009", *Science*, 333(1093), DOI: 10.1126/science.1199169.

1
2
3
4
5
6
7
8
9
10
11
12
13
14
15
16
17
18
19
20
21
22
23
24
25
26
27
28
29
30
31
32
33
34
35
36
37
38
39
40
41
42
43
44
45
46
47
48
49
50
51
52
53
54
55
56
57
58
59
60
61
62
63
64
65

Table 1. Non-linear correlations (R^2) between zonal monthly NPP predicted by the CASA model and zonal monthly input parameters of surface air temperature (TMP), precipitation (PPT), and MODIS EVI values. Correlations between monthly anomalies (2000-2009) and predicted monthly NPP anomalies are shown in parentheses.

Latitude Zone	TMP	PPT	EVI
90° – 60° N	0.94 (0.04)	0.71 (0.03)	0.77 (0.53)
60° – 30° N	0.95 (0.12)	0.71 (0.01)	0.88 (0.61)
30° – 0° N	0.79 (0.05)	0.83 (0.01)	0.79 (0.26)
0° – 30° S	0.70 (0.14)	0.93 (0.02)	0.73 (0.51)

Table 2. Comparison of the tropical rainforest zone NPP (Pg C) totals in 2009 between the CASA model and the MNA (Zhao and Running, 2010)

Continent	CASA	MNA
Africa	2.45	2.87
Asia	3.74	3.81
South America	6.53	7.52
Total Rainforest	13.7	15.6

Figure captions

Figure 1. Comparison of observed NPP ($n = 1927$; Olson et al., 1997) to predicted annual values from the CASA model, driven separately by (a) MODIS-EVI and (b) MODIS-FPAR monthly inputs for the year 2001. The 1:1 regression line on each graph is shown, along with the linear correlation coefficient for the best fit to that 1:1 line.

Figure 2. Frequency distribution of annual NPP from (a) 38 old-growth tropical forest measurement sites compiled by Clark et al. (2001), and (b) tropical forest pixels ($n = 6620$) in the CASA model 0.5° latitude/longitude global grid.

Figure 3. Comparison of CASA monthly NPP to Ameriflux measurements derived from eddy-correlation estimates of the corresponding monthly NPP fluxes. Ameriflux NPP fluxes were plotted within an uncertainty range of 40% to 50% of GPP carbon flux.

Figure 4. Scatter plot of Ameriflux tower estimates of monthly NPP and CASA predicted NPP values for the same months.

Figure 5. Interannual variations from 2000 through 2009 in anomalies of annual total NPP for the CASA model for the Northern Hemisphere (NH - green circles) and the Southern

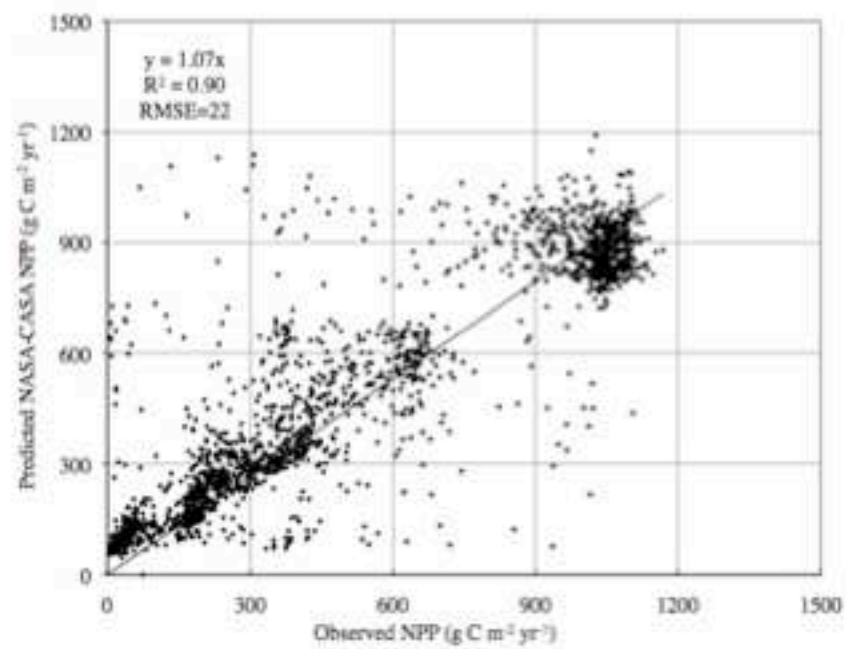
1
2
3
4 Hemisphere (SH - red circles). Global total NPP amounts are shown above the line plot in units
5
6 of Pg C yr⁻¹ (1 Pg = 10¹⁵ g).
7
8
9

10
11 Figure 6. Spatial pattern of terrestrial NPP linear trends from 2000 through 2009.
12
13
14

15
16 Figure 7. Global maps of annual NPP anomalies (2001 – 2009) derived from subtraction of the
17
18 decadal mean NPP values from the CASA model. Extensive negative NPP anomalies in the
19
20 following years were observed: 2001-2002 across the central United States, southern Africa,
21
22 China, and eastern Brazil associated with severe drought in these regions; 2003-2004 across most
23
24 of Europe and eastern Russia associated with extreme summer heat; 2005 across the southern
25
26 Amazon and central Africa associated with severe drought, 2007-2009 across the southeastern
27
28 United States, east Africa, and Australia associated with severe drought (World Meteorological
29
30 Organization, 2001-2009).
31
32
33
34
35
36
37
38
39
40
41
42
43
44
45
46
47
48
49
50
51
52
53
54
55
56
57
58
59
60
61
62
63
64
65

Fig 1.

a) MODIS EVI 2001



b) MODIS FPAR 2001

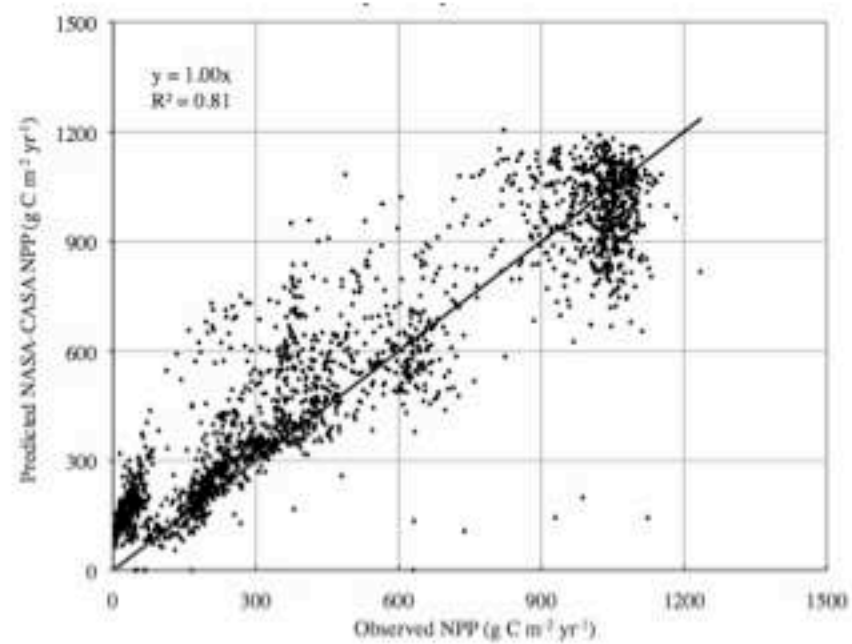


Fig 2.

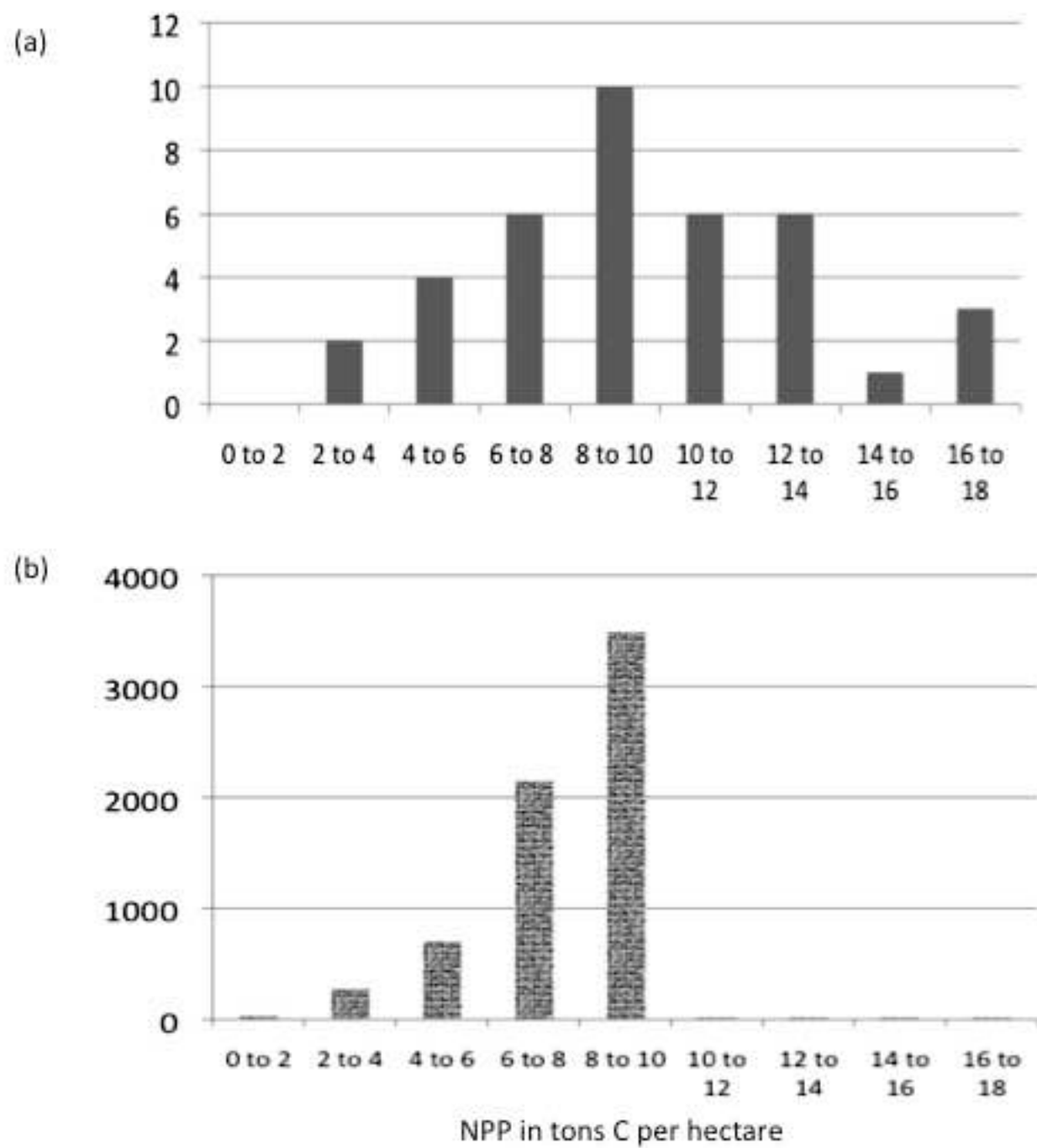
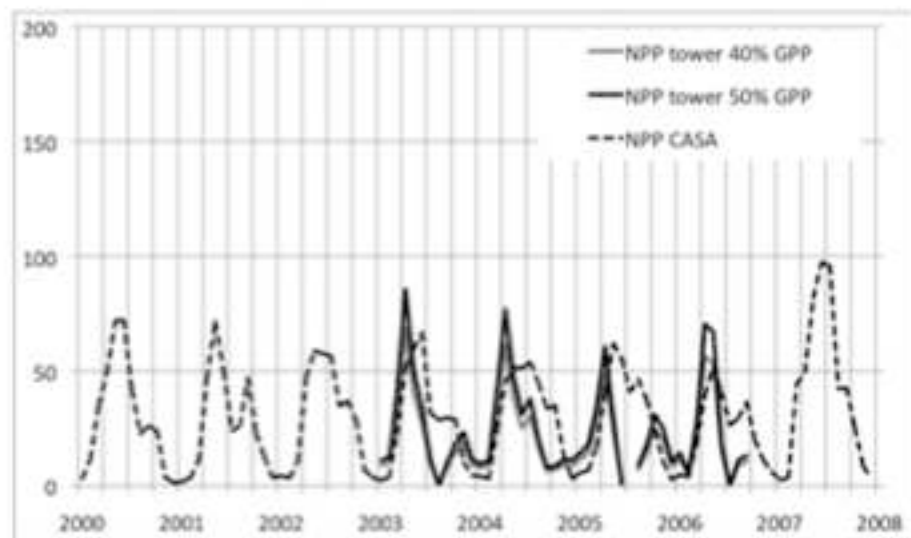


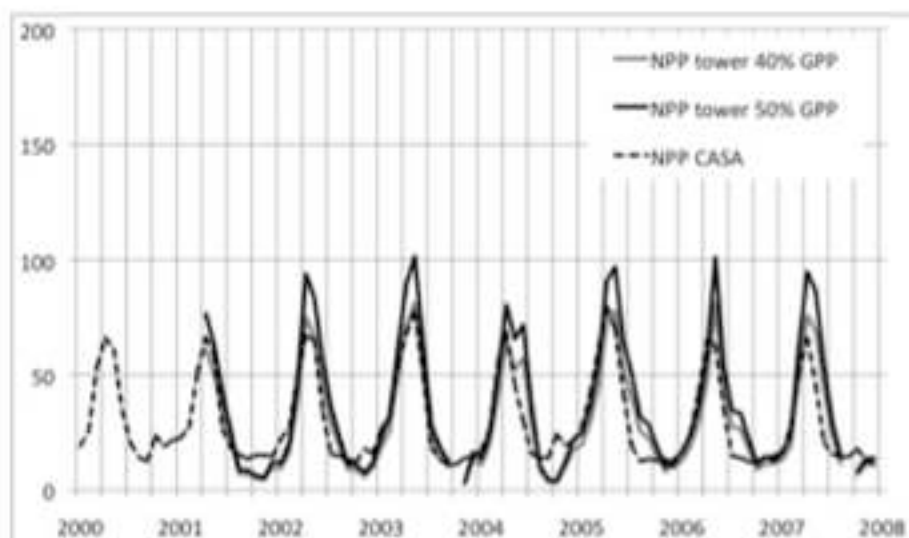
Figure 3
[Click here to download high resolution image](#)

Fig 3.

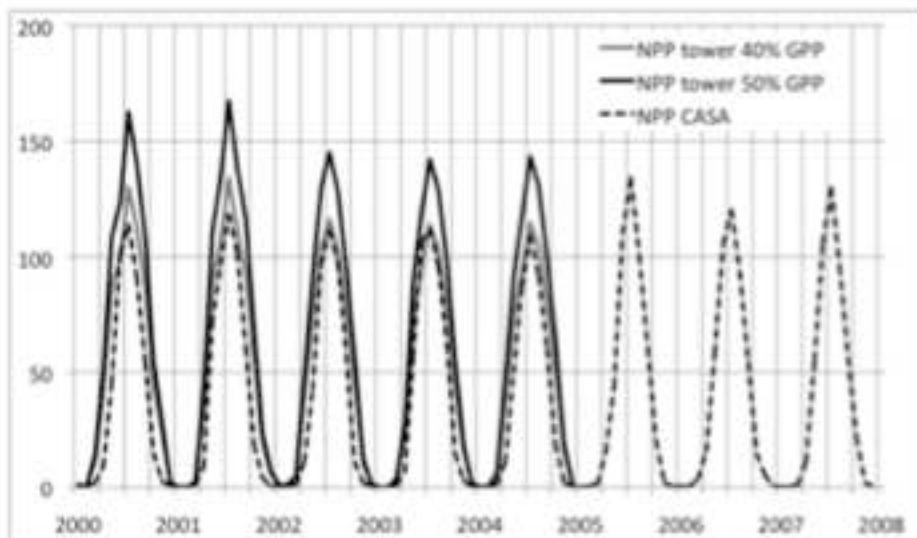
a. ARM SGP Mixed Cropland



b. Tonzi Savanna Grassland



c. Howland Mixed Forest



d. Bartlett Deciduous Broad-leaf Forest

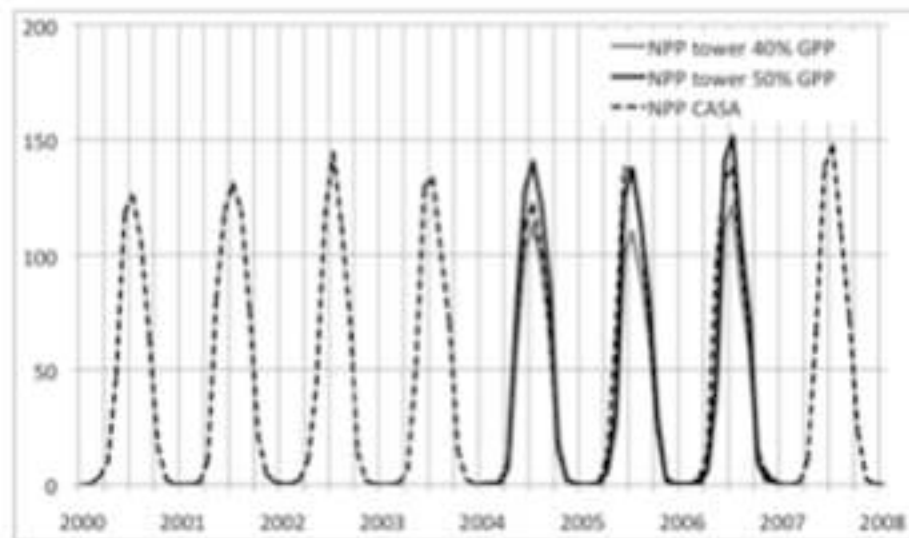
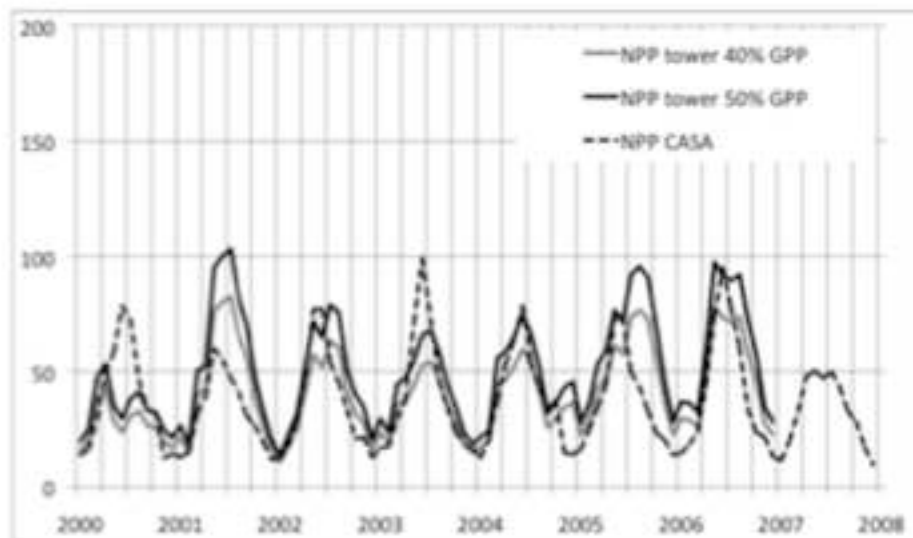


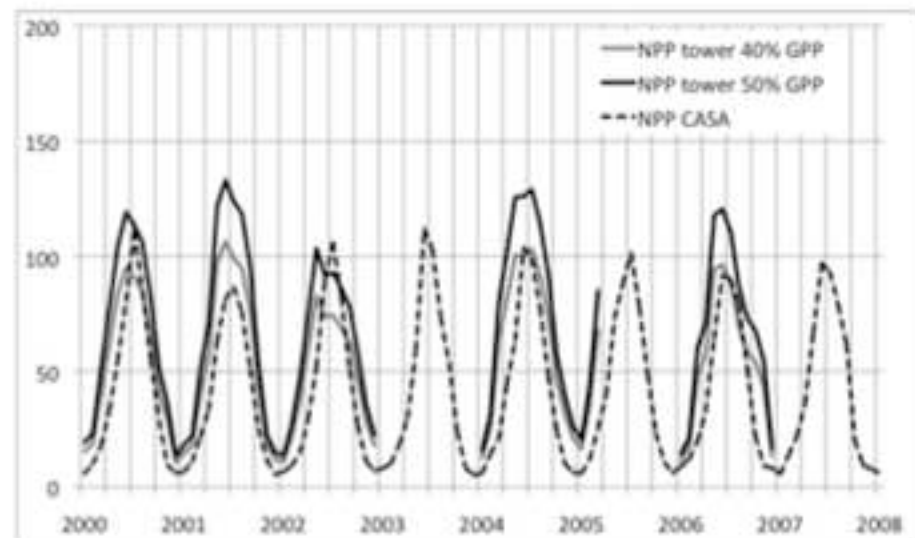
Figure 3b
[Click here to download high resolution image](#)

Fig 3.

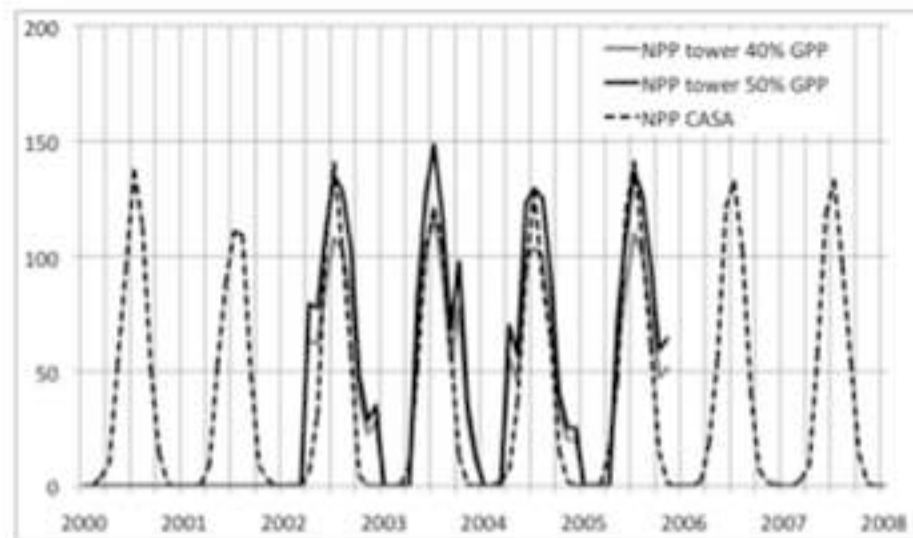
e. Blodgett Evergreen Needle-leaf Forest



f. Wind River Evergreen Needle-leaf Forest



g. Wisconsin Mixed Forest



h. Tapajos Evergreen Broad-leaf Forest

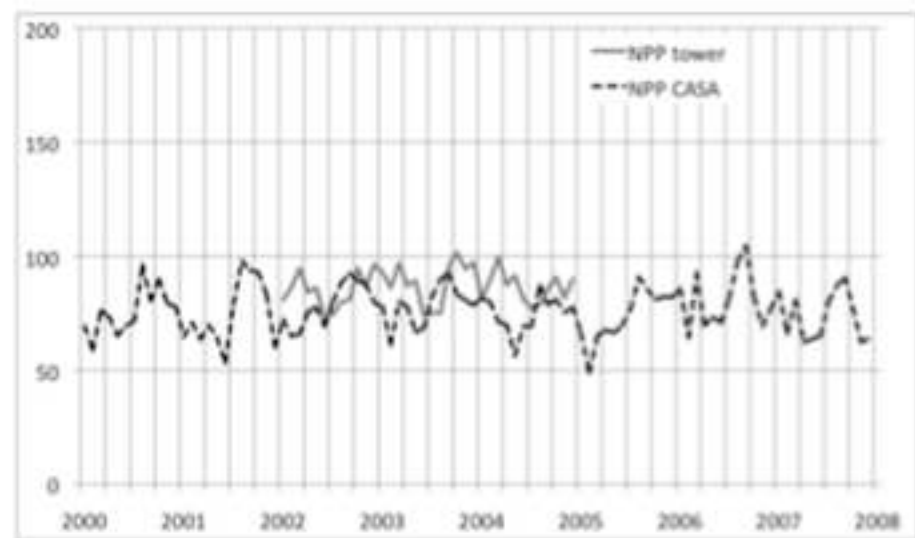


Figure 4
[Click here to download high resolution image](#)

Fig 4

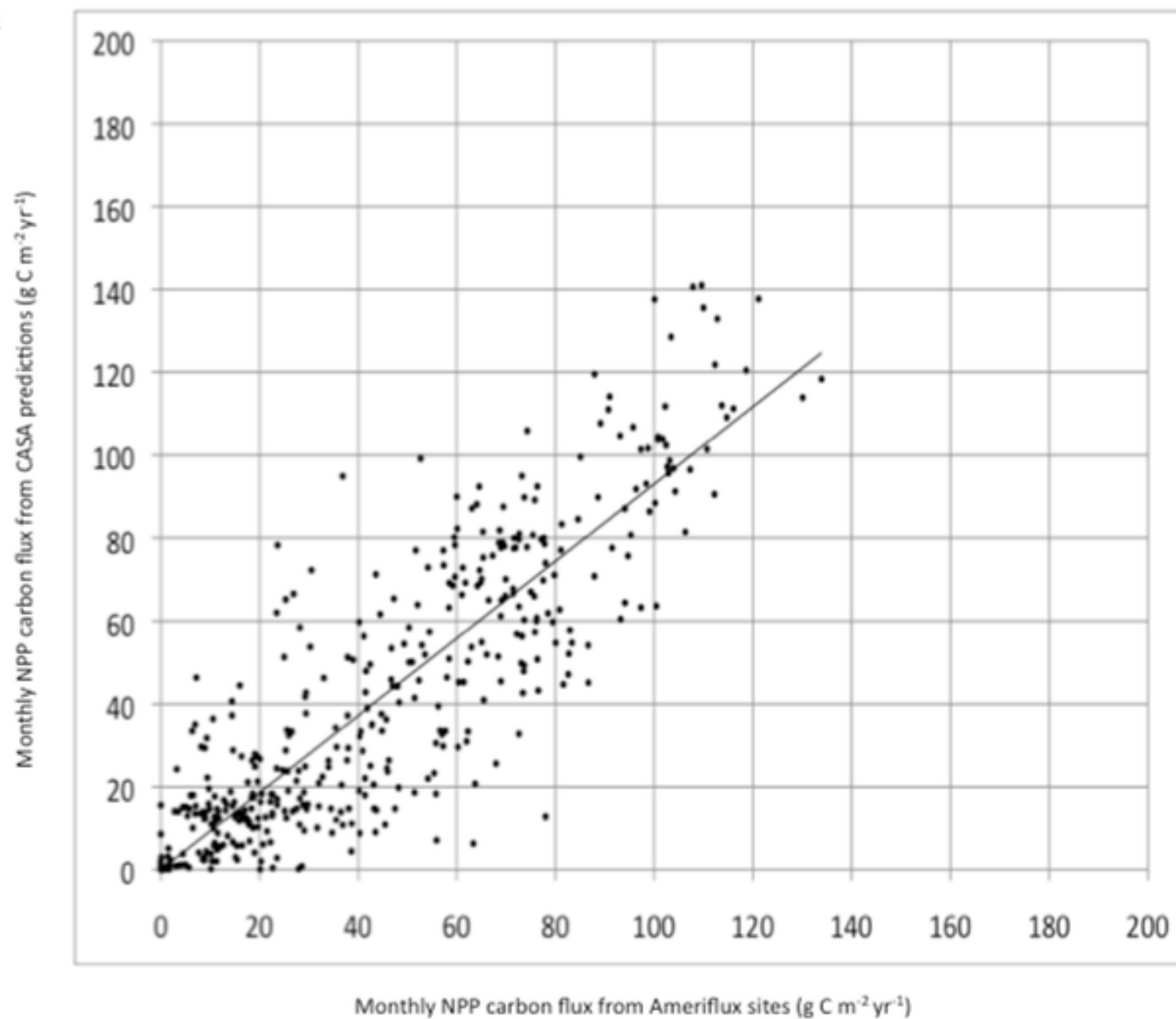


Fig 5.

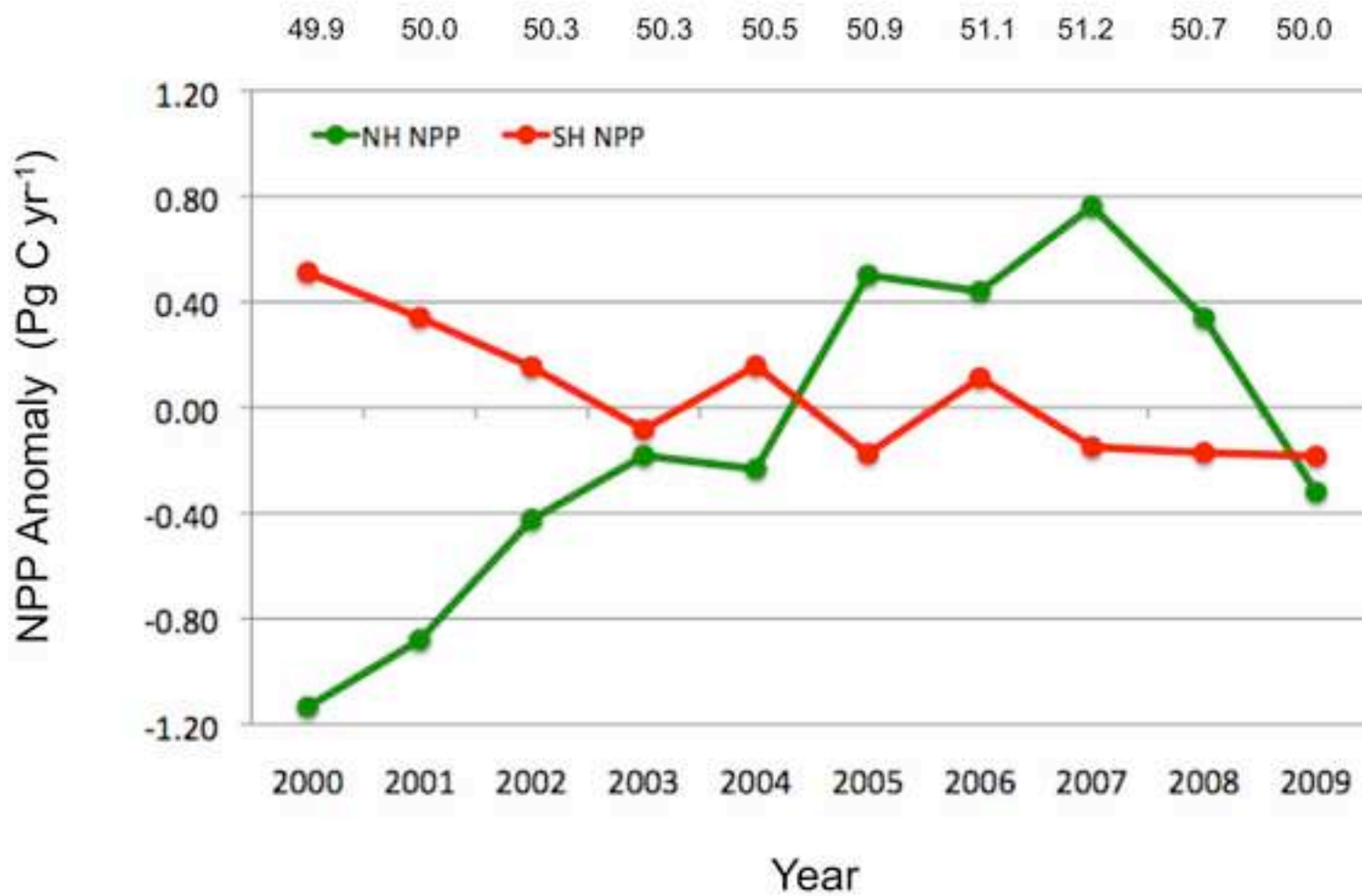


Fig 6.

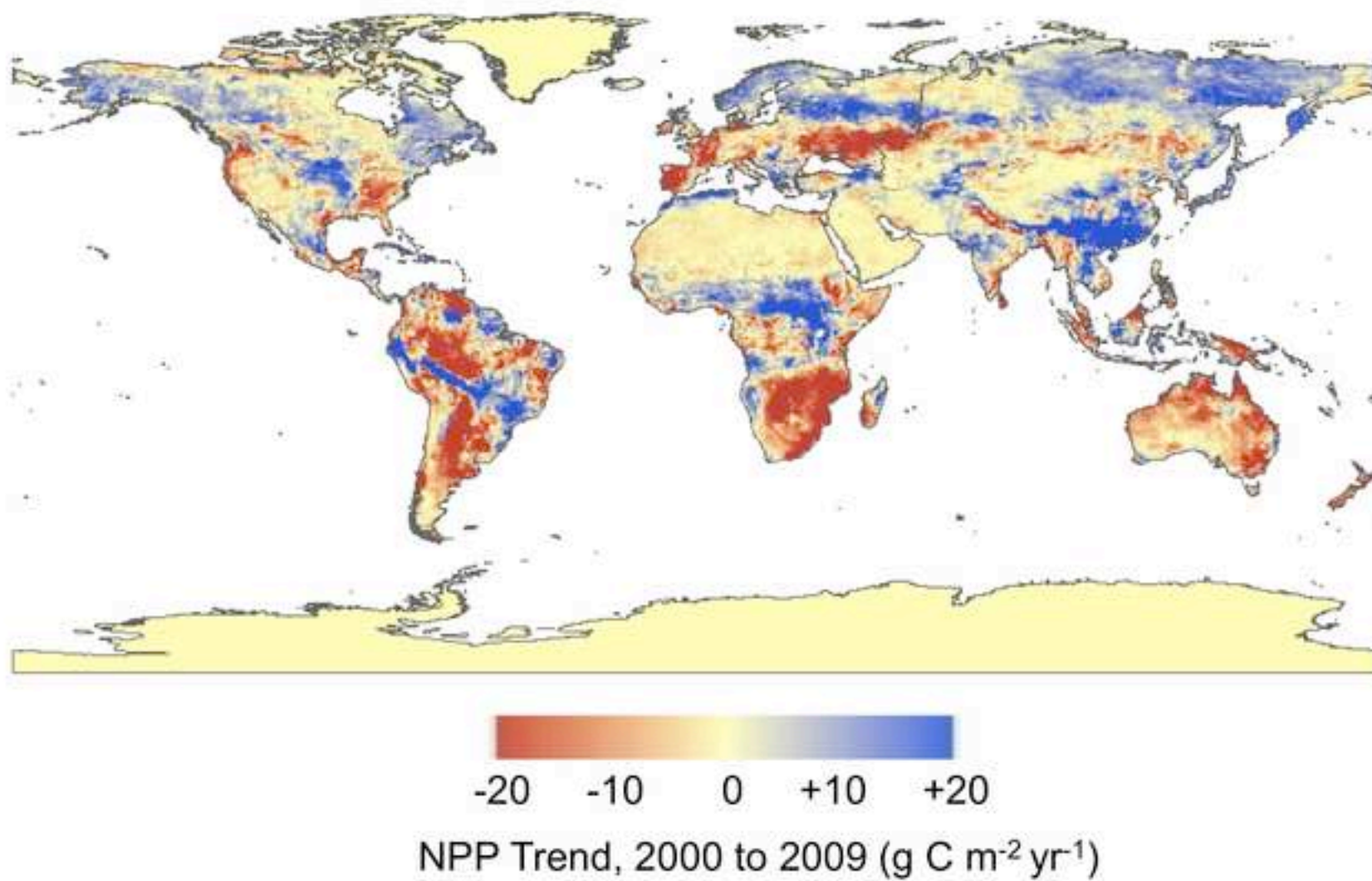


Figure 6b
[Click here to download high resolution image](#)

Fig 7.

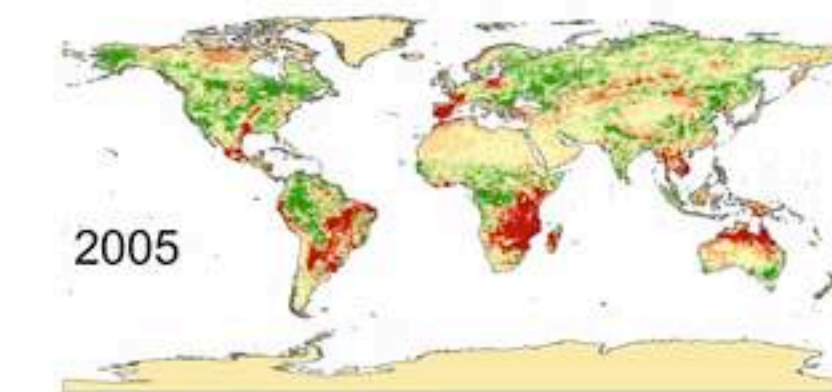
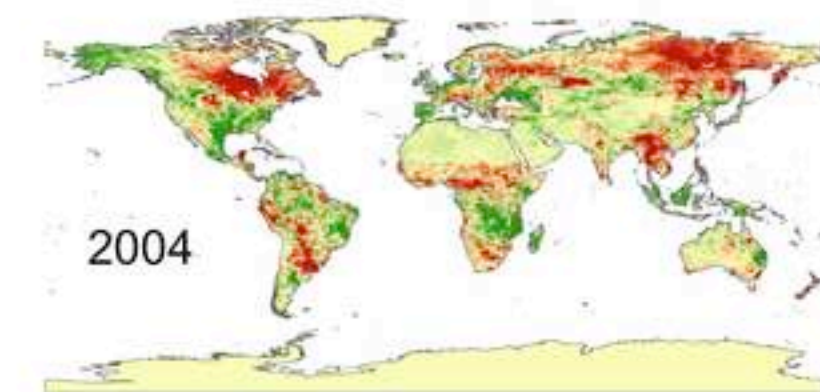
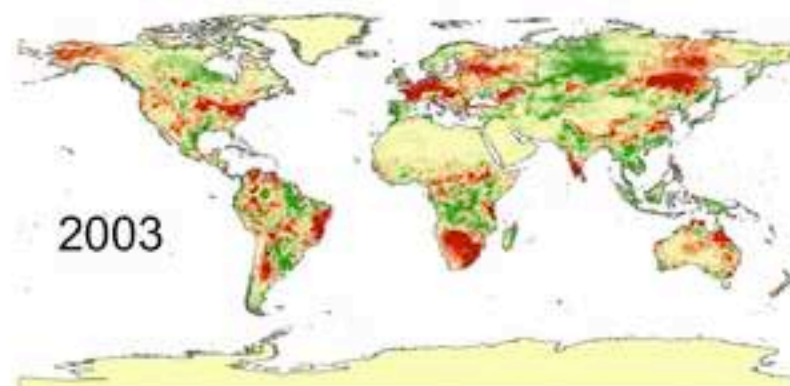
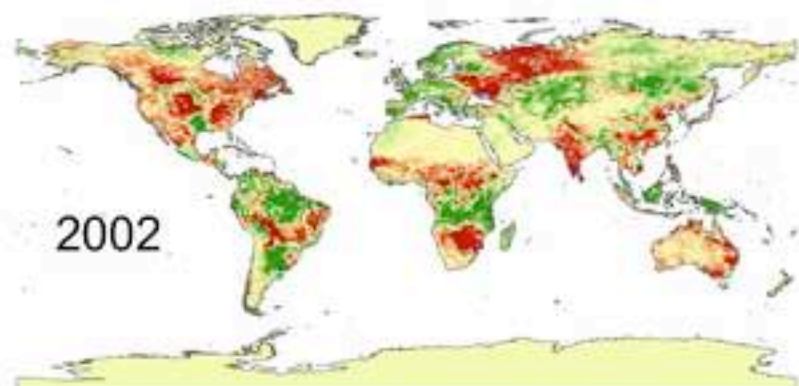
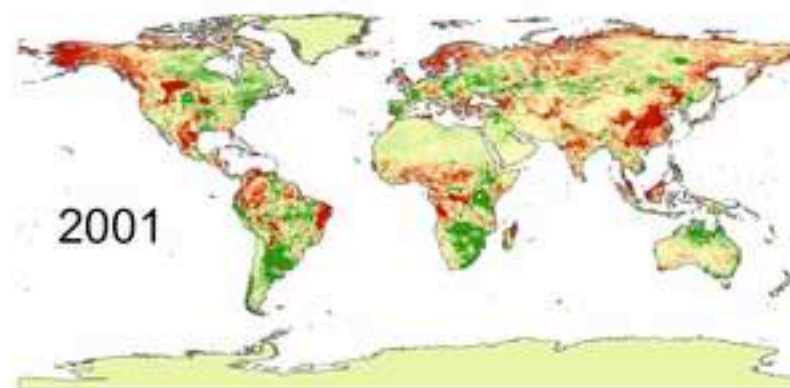
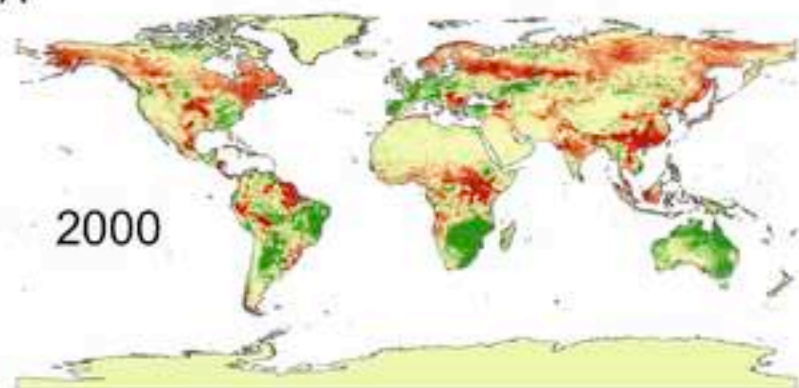


Fig 7.

